International Journal of Engineering &Technology, 7 (1.8) (2018) 103-107

International Journal of Engineering & Technology

Website: www.sciencepubco.com/index.php/IJET

Research paper

Rotor autocentering and speed control of hybrid bearingless SRM using single-neuron adaptive PID controller

Polamraju. V. S. Sobhan [1]*, G. V. Nagesh Kumar [2], P. V. Ramana Rao [3]

[1] *Department of EEE, VFSTR, Guntur, India*
[2] *Department of EEE, Vignan's Institute of Information Technology, Visakhapatnam, India*
[3] *Department of EEE, Acharya Nagarjuna University, Guntur, India*
**Corresponding author E-mail: pvssobhan@gmail.com*

Abstract

The bearingless switched reluctance motor (BLSRM) is emerging as an attractive option for modern industrial applications because of the features, such as compact size, lubrication and seal free performance, long life and ability to rotate at very high speed and high power. The control approach is extremely fundamental to a steady operation because of its highly nonlinear, multi variable and open loop unstable nature. This paper presents a single neuron based rotor suspension control of a 12/14 Hybrid Pole BLSRM with autonomous rotation and suspension poles. This hybrid pole structure produces the suspension force linearly with respect to rotor position and independent of the torque characteristics. Implementation of a non model based Single neuron adaptive PID Controller by avoiding the modeling complexity is proposed. Experimental results demonstrate that the proposed controller maintains the rotor in the center position as well as the speed tracking and disturbance elimination performances independently.

Keywords: *BLSRM; Eccenrtric Control; Suspension Control; Single-Neuron; PID Controller.*

1. Introduction

High-speed motors are required in modern industrial applications such as turbo molecular pumps, centrifugal pumps, compressors and so on [1-3]. The traditional mechanical bearing which is in contact and bears the shaft of the high speed motor creates many problems such as mechanical wearing, thermal problem, increasing of frictional drag, and decrease in service life of bearings. Moreover the use of lubricants, and seals makes the motor not suitable for high purity environments such as space, semiconductor, pharmaceutical, and radioactive [4-5]. To overcome the limitations of the conventional bearing motors, magnetic-bearing motors (or bearingless motors) which combines torque driving and self-levitation, have been designed [6-7].

A bearingless motor is a motor integrated with magnetic bearing, with many benefits, such as compact size, lubrication and seal free performance, long life, low cost and assists the motor to rotate at very high speed and high power [8-9]. The switched reluctance motors are a natural choice as bearingless motors because of the magnetic attraction between the stator and rotor poles produces the torque to drive the rotor. In addition the rotor experiences a high amount of radial force which can be used effectively for suspension the rotor shaft.

The flux distribution in the air gap is irregular due to excitation of the suspension winding and the regulation of rotor eccentricity is achieved by suspension force. The magnetic suspension force and torque can be created in a same unit and their control is carried out with less number of power electronic converters, controllers, and connection wires when contrasted with a motor having magnetic bearings

The majority of the proposed bearingless switched reluctance motor (BLSRM) structures are based on conventional SRM structure, which complicates the rotor eccentricity control due to the existence of coupling between the suspension force control and the torque control. M. Takemoto et.al proposed differentially wounded BLSRM in which auxiliary suspension windings and torque windings are wound on stator poles and are controlled by different power converters [10-11]. In the hybrid rotor structure proposed by Morrison et.al the rotor is made up of two laminated segments, circular segment used for suspension and multipole segment used for both suspension and torque generation [12]. In all the aforesaid designs, as the control of torque is coupled with suspension force they cannot guarantee the full utilization of generating torque and radial force regions and selection of operating point is a compromise between the two forces. Wang, H et.al proposed a hybrid BLSRM by separating suspension force pole with torque pole to minimize the inter-dependency of two forces. Due to this decoupling poles, the suspension force control can be achieved easily [13].

The Suspension control of the hybrid BLSRM rotor is quite a challenging problem due to its inherently high nonlinearity and uncertainty. Zhenyao Xu et.al proposed one PI controller for the speed tracking and two independent PID Controllers for controlling the rotor displacement in x and y directions. The tuning of the PID controller parameters is a time consuming process and poor tuning results rotor eccentricity, torque pulsations and hence speed ripples due to high nonlinear variation of each phase inductance [14].

The design of suitable control system for the rotor autocentering of BLSRM in view of decoupling is critical for true operation of a BLSRM.The parameters of conventional PID controllers used to control the rotor autocentering, have the fixed values when the motor operating in a specific state. Whenever the motor parameters or state changes, the performance will be influenced, and the dynamic and steady state accuracy cannot be guaranteed. Similar-

ly, it is exceptionally troublesome for this control scheme to get an adequately high-performance control to the BSRM system, which is a, nonlinear- multivariable and strongly coupling system with time-dependent parameters.

In this paper, a single neuron adaptive based PID Controller is proposed for rotor suspension and speed control of 12/14 hybrid pole type BLSRM. Two independent non model based SNAPID controllers proposed for suspension force control and the torque control by avoiding the modeling complexity are proposed [15-17]. To analyse the rotor eccentricity control and speed tracking performances experimentation is performed on the proposed BLSRM.

2. Hybrid pole 12/14 BLSRM

2.1. Structure

The typical structure of 12/14 hybrid stator pole type BLSRM shown in Fig.1. The 12 stator poles are wound with two different windings, 8 poles for torque production and 4 poles for suspension force. This arrangement helps to decouple the torque from suspension force. Since the suspension force pole arc is made slightly more than one rotor pole pitch, the available overlap area between rotor and suspension force pole becomes constant, compared with conventional bearingless SRM. This design completely decouples the suspension force control from torque control due to negligible undesirable torque produced by suspension force poles. The rotational torque produced by A and B phases, which are formed by connecting 4 torque pole windings P_{A1}, P_{A2}, P_{A3} and P_{A4} in series and other 4 torque pole windings P_{B1}, P_{B2}, P_{B3} and P_{B4} in series respectively. The torque control can be achieved by controlling two phase currents i_A and i_B.The x-directional suspension force is produced by the suspension pole winding currents i_{xp} and i_{xn} flowing in two suspension force poles P_{xp} and P_{xn}. Similarly the y-directional suspension force is produced by the suspension pole winding currents i_{yp} and i_{yn} flowing in two suspension poles P_{yp} and P_{yn}. The suspension force on the rotor in positive and negative directions of both x and y directions, can be controlled by controlling i_{xp}, i_{xn}, i_{yp} and i_{yn} independently.

P_A

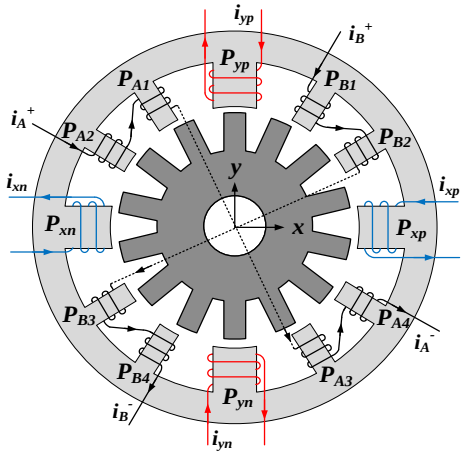

Fig. 1: Hybrid BLSRM Pole Structure.

Fig. 2 demonstrates the dependency of torque and levitation force of BSRM. The viable region of torque is from position 1 to 3 and accessible levitation force starts from position 2 to 4. From positions 2 to 3, the overlapping of torque and levitation force occurs and this region is highly suitable for the motor to generate sufficient torque and levitation force in the meantime. This region is extremely thin due to the fundamental nature of torque and levitation force generation. So the working point must be chosen to trade off amongst torque and levitation force when utilizing the regular structure and full utilization of torque and levitation force regions is not possible. Hence to acquire enough levitation the increase in current in essential and dwell angle ought to be shifted towards aligned position. This leads in increased copper loss and thermal issues because of the increase in current value to get higher torque or levitation force. But with the common winding current the simultaneous generation of torque or levitation force happens and are non linearly depends on current and position. In this manner, it is extremely hard to decouple the torque from levitation force.

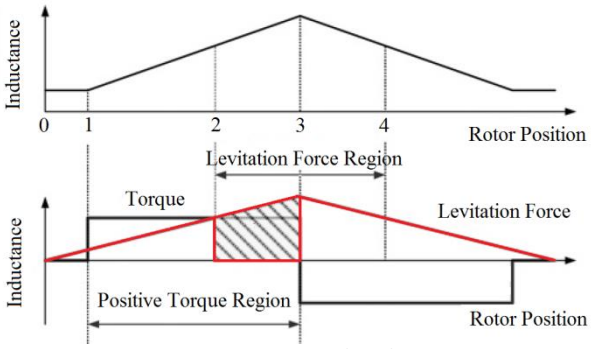

Fig. 2: Inductance Profile of SRM.

2.2. Torque control

The electromagnetic torque produced by torque poles P_A and P_B, is proportional to the square of the phase current and derivative of inductance with respect to rotor position as given in equation 1 and the torque profile mainly depends on the inductance profile.

$$T = \frac{1}{2} i^2 \frac{dL}{d\theta} \tag{1}$$

In the BLSRM, the suspension force winding inductance profile is nearly constant with the constant current hence the inductance change with rotor position is negligible and the torque is independent of suspension force current. In case of the torque winding, the change in the inductance with respect to rotor position is very large due to due to large variation in the inductance profile from aligned to unaligned position hence the total torque on the rotor is due to torque winding only.

2.3. Suspension force control

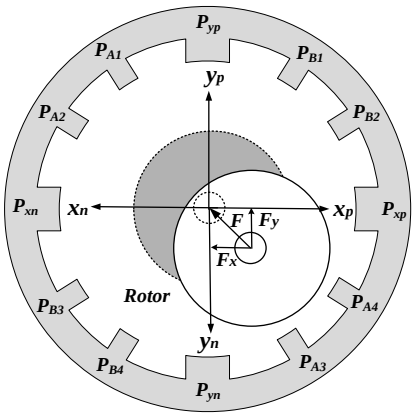

Fig. 3: Eccentricity Effect of the Air-Gap Displacement.

The absence of mechanical bearings in BLSRM causes displacement of the rotor from the center position and eccentricity effects. Fig. 3 shows the rotor eccentricity due to unbalanced pull force directed in the fourth quadrant of x-y plane and the required compensating suspension force F on the rotor which is in the direction of second quadrant. The rotor movement towards the central position is controlled by the controller using the signals from the power amplifier and the four displacement sensors which detects the rotor eccentricity. The net suspension force F is the resultant of F_x

and F_y, where F_x is the generated suspension force in negative x-direction due to the winding current i_{xp} in pole P_{xn} and F_y is the generated suspension force in positive y-direction due to the winding current i_{yp} in pole P_{yp}. The magnitude of F in any desired direction can be controlled by regulating the values of four suspension force winding currents i_{xp} , i_{xn} , i_{yp} and i_{yn}.

3. Single neuron adaptive PID control

The structure of PID controller combined adaptive single neuron with and adjustable weights with self-learning is shown in fig.4.

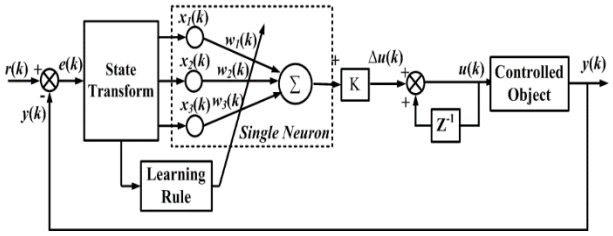

Fig. 4: Block Diagram of Single Neuron PID Control System.

The error between the reference input r (k) and actual output y (k) is converted into three input variables of the single neuron as given in (2)

$$\begin{aligned} x_1(k) &= e(k) = r(k) - y(k) \\ x_2(k) &= \Delta e(k) = e(k) - e(k-1) \\ x_3(k) &= \Delta^2 e(k) = e(k) - 2e(k-1) + e(k-2) \end{aligned} \tag{2}$$

The incremental output of the single neuron is expressed as

$$\Delta u(k) = u(k) - u(k-1) = K \sum_{i=1}^{3} \frac{x_i(k) w_i(k)}{\sum_{i=1}^{3} |w_i(k)|} \tag{3}$$

Where u (k) is the output and K is the positive scale factor of the single neuron. The self-learning of the single neuron is implemented by adjusting weights w_i (k), i=1, 2, 3 using supervised Hebb's learning and the updated weights are given by equation (4).

$$\begin{aligned} w_1(k+1) &= w_1(k) + \eta_I K z(k+1) u(k) x_1(k) \\ w_2(k+1) &= w_2(k) + \eta_P K z(k+1) u(k) x_2(k) \\ w_3(k+1) &= w_3(k) + \eta_D K z(k+1) u(k) x_3(k) \end{aligned} \tag{4}$$

where $z(k+1) = e(k+1)$ and η_I ,η_P and η_D are learning constants of integral, proportional and differential parts respectively, which are used to modulate the different weights w_i(k).

The rules for determining the adjustable parameters K, η_I, η_P and η_D are

1) If the step response contains large overshoot and oscillations then K should be reduced , if the response is without overshoot and large rise time then K should be increased and in both conditions the three learning rates are unchanged
2) If the response contains frequent sine attenuation, then reduction in ηP is required keeping the other parameters unchanged.
3) If the speed of the response is fast and contains large overshoot, then reduction in ηI is required while keeping the other parameters unchanged.
4) If the speed of the response is slow, ηI is required to increase, and if contains large overshoot corresponding increase in ηP is required while keeping the other parameters unchanged.
5) The initial value of ηD is to be small and the adjustment should be gradual.

The Fig 5 illustrates how the 12/14 BLSRM's suspension and speed control are achieved simultaneously based on decoupled suspension force and torque.

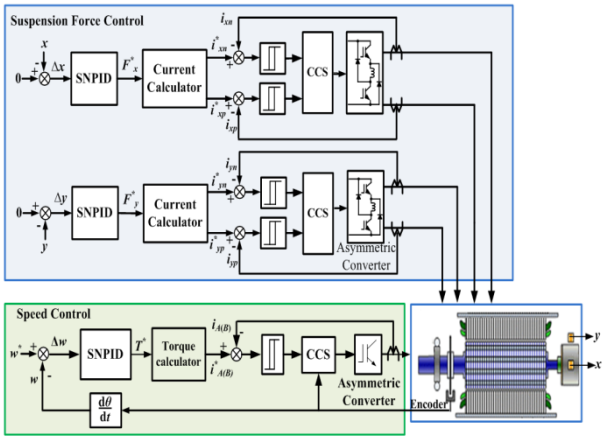

Fig. 5: SNAPID Control Scheme for BLSRM.

The rotor radial position control is achieved by adopting two independent SNAPID controllers in x and y directions. The rotor position in both directions (x and y) is sensed by four eddy current displacement sensors and the angular displacement of the rotor is sensed by an encoder. The two controllers generate the required suspension forces $F_x^*$and F_y^* to drive the rotor to the center using the error between the detected rotor radial displacement and the reference value x^* and y^* in both the directions. For any rotor position, two suspension poles in x and y directions (P_{xp}, P_{xn} , P_{yp} and P_{yn}) and corresponding currents (i_{xp} , i_{xn} , i_{yp} and i_{yn}) are selected using lookup table as shown in table 1.

Table 1: Look up Table

Desired force	Selected suspension force poles
$+F_x$ and $+F_y$	P_{xp} and P_{yp}
$+F_x$ and $-F_y$	P_{xp} and P_{yn}
$-F_x$ and $+F_y$	P_{xn} and P_{yp}
$-F_x$ and $-F_y$	P_{xn} and P_{yn}

The currents of selected suspending pole windings are controlled by the current regulated PWM to generate the switch signals of asymmetric converter. The motor speed is regulated by controlling torque using a SNAPID controller, whose input is the difference between the reference and the speed detected from encoder. The speed controller output is the PWM duty ratio to turning on and turning off of the switches in asymmetric converters of corresponding torque winding phase.

4. Experimental results

To validate the potency and superiority of the SNAPID control, experiments have been performed on Hybrid pole type BLSRM and the experimental test setup it is shown schematically in Fig. 6. The proposed control scheme is implemented with TMS320F2812 DSP which is compatible with Matlab/Simulink and includes four dual PWM channels, 4 ADCs and a speed encoder input. The designed parameters of SNAPID controller are shown in table 2.

Table 2: Tuned Parameters of SNAPID Controller

Parameter	Values
Learning constants	η_I= 0.6 , η_P= 1.0 , η_D= 0.8
Scale factor	K=1
Initial weights	w_1= w_2= w_3=0.5

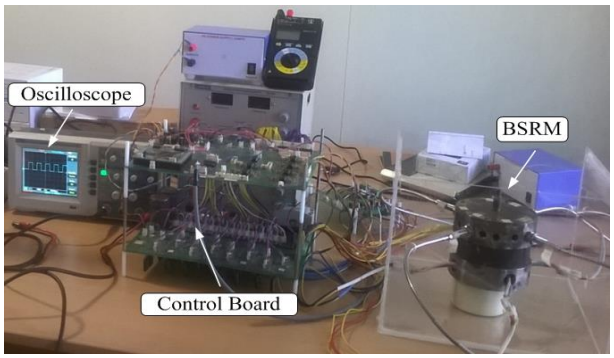

Fig. 6: Experimental Setup.

4.1. Rotor suspension force control from the rest

The experimental results of rotor displacements in both directions (x and y) and corresponding suspension force currents when the rotor is stationary are shown in fig.7. From the fig. 7(a), it can be seen that, the rotor is initially located at 75 µm in the negative x direction and 65 µm in the negative y direction, when SNAPID controlled suspension force is applied, the rotor rises steadily to the centre of the stator. Fig. 7(b) shows that the change in suspension winding currents when the rotor is suspended from rest. Since the torque winding control is not applied the current and the rotor speed is zero.

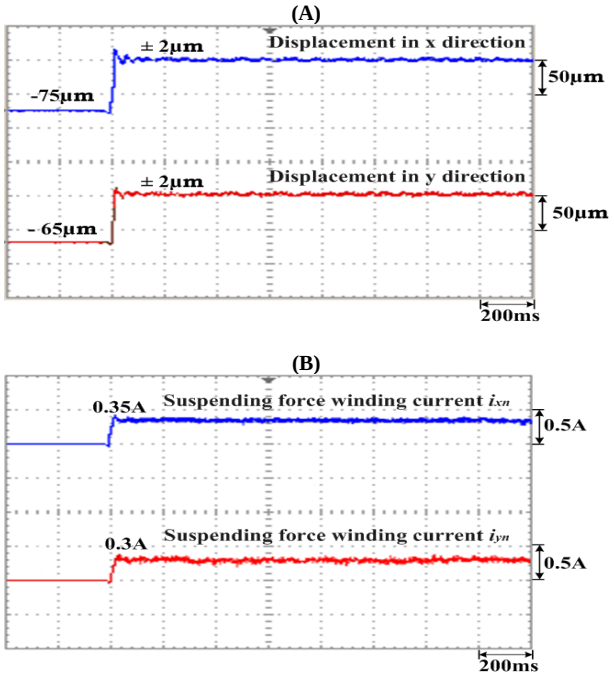

Fig. 7: (A) Rotor Displacements and (B) Suspension Winding Currents under Standstill Conditions.

4.2. Variation in speed

Fig.8 displays the results of the suspension and torque control when the rotor speed is suddenly changes from rest to 1000 rpm at 0.4 sec. As shown in fig. 8(a), the torque winding current of phase A (Similarly phase B) rises suddenly and settles when the speed of the motor is varied. From fig. 8 (b) and 8 (c), it can be observed that the rotor suspends steadily with negligible eccentric error, before and after change in speed occurs and the change in suspension winding currents magnitude remains same.

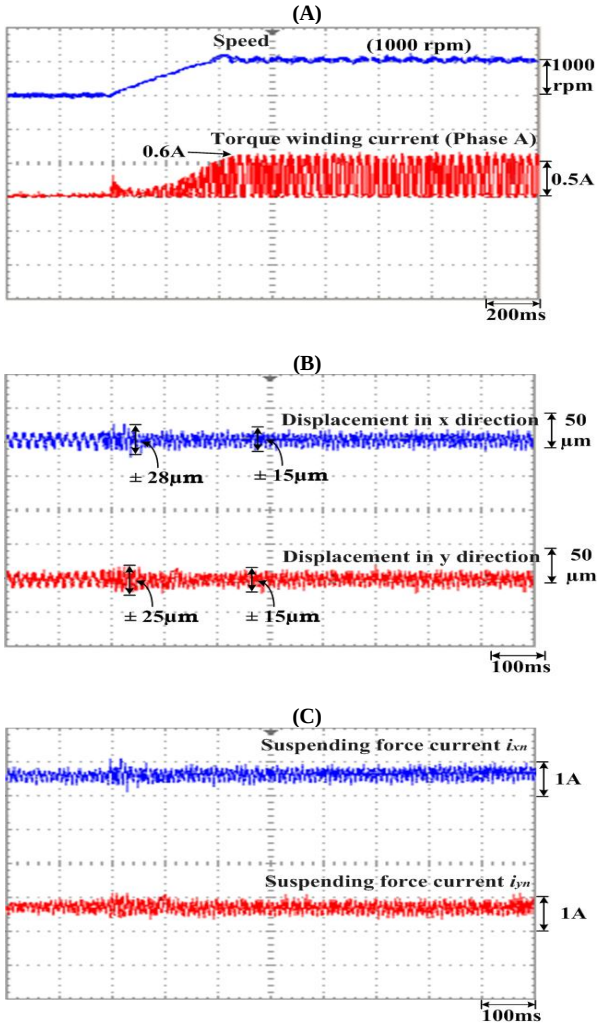

Fig. 8: (A) Speed and Torque Winding Current (B) Rotor Displacements and (C) Suspension Winding Currents When the Speed Is Varied.

4.3. Variation in load

Fig. 9 shows the experimental results of suspension and torque control under variable load conditions at constant speed. As shown in the fig.9(a), when a 2 N.m load is applied at 0.4 sec, the torque winding current of phase A (Similarly phase B) increased a little to overcome it, however, the variation in the motor speed is very little. As shown in the fig. 9 (b) the rotor had an eccentricity at the time when the load is changed, but it restores quickly to the center. It explains that, the variation in the load has almost no effect on the suspension force. Fig. 9 (c) shows that the change in the magnitude of suspension winding currents when the rotor is loaded at 0.4 sec.

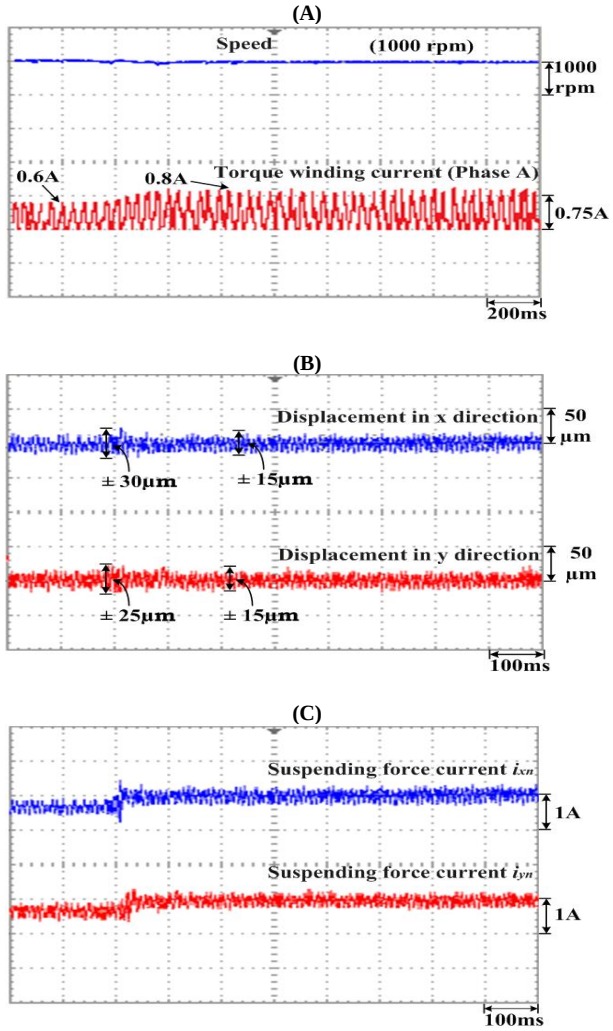

Fig. 9: (A) Speed and Torque Winding Current (B) Rotor Displacements and (C) Suspension Winding Currents When the Load Is Varied

5. Conclusion

The hybrid pole type BLSRM is a nonlinear system with unavoidable parameter variations has the inherent advantage of strong decoupling between rotational force and the suspension force which facilitates the independent control of rotor suspension and torque developed. This paper proposes a control scheme combing the conventional PID control with artificial neuron for Hybrid pole type BLSRM. The suspension control is achieved by two single neuron adaptive PID controllers and one for speed control. The online adjustment of PID gains can be achieved by single neuron with three inputs based on unsupervised Hebb algorithm. The experimental results establish that the steady suspension of rotor at the centre of the stator from rest, variable load and speed conditions by adjusting the weights of the single neuron.

References

[1] Z. Y. Xu, F. G. Zhang, and J. W. Ahn, "Design and analysis of a novel 12/14 hybrid pole type bearingless switched reluctance motor," in Proc. IEEE ISIE, 2012, pp. 1922–1927.

[2] M. Ooshima and C. Takeuchi, "Magnetic suspension performance of a bearingless brushless DC motor for small liquid pumps," IEEE Trans. on Industry Applications, vol. 47, no. 1, Jan. 2011, pp. 72-78. https://doi.org/10.1109/TIA.2010.2091233.

[3] Y. Okada, N. Yamashiro, K. Ohmori, "Mixed flow artificial heart pump with axial self-bearing motor," IEEE/ASME Trans. on Mechatronics, vol. 10, no. 6, Dece. 2005, pp. 658-665.

[4] R. Bosch, "Development of a bearingless electric motor," in Proc. ICEM, Pisa, Italy, 1988, pp. 373–375.

[5] J. Bichsel, "The bearingless electrical machine," in Proc. Int. Syposium on Magnetic Suspension Technology, Hampton, VA, USA, 1991, pp. 561–573.

[6] J. X. Shen, K. J. Tseng, D. M. Vilathgamuwa, and W. K. Chan, "A novel compact PMSM with magnetic bearing for artificial heart application," IEEE Trans. Ind. Appl., vol. 36, no. 4, Jul./Aug. 2000, pp. 1061–1068. https://doi.org/10.1109/28.855961.

[7] L. Hertel, W. Hofmann, "Basic approach for the design of bearingless motors," Proc. of the 7th Int. Sym. on Magnetic Bearings, August 2000.

[8] S. Ayari, M. Besbes, M. Lecrivain, and M. Gabsi, "Effects of the airgap eccentricity on the SRM vibrations," in Proc. Int. Conf. Elect. Mach. Drives, 1999, pp. 138–140. https://doi.org/10.1109/IEMDC.1999.769052.

[9] D. H. Lee and J.W. Ahn, "Design and analysis of hybrid stator bearingless SRM," J. Elect. Eng. Technol., vol. 6, no. 1, 2011, pp. 94–103. https://doi.org/10.5370/JEET.2011.6.1.094.

[10] M. Takemoto, A. Chiba, H. Suzuki, et al., "Radial Force and Torque of a Bearingless Switched Reluctance Motor Operating in a Region of Magnetic Saturation," IEEE Trans. on Industry Application, Jan./Feb.2004, 40 (1): 103-112. https://doi.org/10.1109/TIA.2003.821816.

[11] M. Takemoto, A. Chiba and T. Fukao, "A New Control Method of Bearingless Switched Reluctance Motors Using Square-wave Currents," Proceedings of the 2000 IEEE Power Engineering Society Winter Meeting, Singapore, CD-ROM, Jan. 2000: 375-380. https://doi.org/10.1109/PESW.2000.849993.

[12] C. R. Morrison, M. W. Siebert, and E. J. Ho, "Electromagnetic forces in a hybrid magnetic-bearing switched-reluctance motor," IEEE Trans. Magn., vol. 44, no. 12, Dec. 2008, pp. 4626–4638. https://doi.org/10.1109/TMAG.2008.2002891.

[13] Huijun Wang, Dong-Hee Lee, Tae-Hub Park and Jin-Woo Abn, "Hybrid stator-pole switched reluctance motor to improve radial force for bearingless application," Energy Conversion and Management,vo1.52, no.2, 2011, pp.1371-1376. https://doi.org/10.1016/j.enconman.2010.09.035.

[14] Zhenyao Xu, Dong-Hee Lee and Jin-Woo Ahn, "Comparative Analysis of Bearingless Switched Reluctance Motors With Decoupled Suspending Force Control", IEEE Transactions on Industry Applications, Vol. 51, No. 1, 2015, pp 733-743. https://doi.org/10.1109/TIA.2014.2331422.

[15] Zhang Yinga, LI Penga and WU Wen-jiangb, "Single Neuron PID Sliding Mode Parallel Compound Control for Alternating Current Servo System," 2012 International Workshop on Information and Electronics Engineering (IWIEE), Procedia Engineering, vol. 29, 2012, pp. 2055 – 2061. https://doi.org/10.1016/j.proeng.2012.01.261.

[16] Xiujia Chen and Hongdi Qiu, "Research on Single Neuron Adaptive PID Controller," applied Mechanics and Materials, Vol. 651-653, 2014, pp. 826-830.

[17] W. D. Chang, R. C. Hwang, J. G. Hsieh, "Stable direct adaptive neural controller of nonlinear systems based on single auto-tuning neuron", Neurocomputing, Vol.48, 2002, pp. 541-554. https://doi.org/10.1016/S0925-2312(01)00627-0.